

Molecular-Dynamics Simulation of Brittle and Ductile Fracture in Amorphous Solids

M.L. Falk

Department of Physics, University of California, Santa Barbara, CA 93106

(December 2, 2024)

Molecular-dynamics simulations of fracture performed in model amorphous solids are shown to exhibit brittle or ductile behavior depending on small changes in interatomic potential. I have developed a measure of non-affine deformation in non-crystalline solids in order to examine plastic flow in the vicinity of the crack. This technique has helped to identify the molecular mechanism of plastic flow and reveals the nucleation of bands of deformation originating at the tip of the ductile crack.

The concepts of brittleness and ductility are central to any understanding of failure in solids. Yet, current theories fall short of describing the dynamics of a transition between these two modes of fracture. The most developed first-principles theories of ductility are rooted in the dynamics of dislocations in crystalline solids [1–3]. These models, however, cannot be valid descriptions of amorphous materials which undergo qualitatively similar transitions between brittle and ductile behaviors. Purely phenomenological theories exist which do not distinguish between crystalline and non-crystalline solids, but these theories have their own shortcomings. Theories involving rate-dependent cohesive zone models [4,5] have recently been shown inadequate for dynamic stability calculations. [6] Other phenomenological approaches to the fracture problem in the context of continuum plasticity are only valid for high velocity cracks in the limit of elastic strain-rate dominance. [7,8]

In order to address these issues, I have carried out a series of molecular-dynamics(MD) simulations of fracture in a simple, two-dimensional amorphous solid. These studies of brittle and ductile behavior are relevant in the context of several different disordered and amorphous materials. The simulated system is similar in some ways to metallic glasses which have been observed to undergo transitions between ductile and brittle behavior both as a function of temperature and due to small amounts of dilute crystallization produced during annealing. [9–11] Similar transitions are also critical to the processing of colloidal ceramic systems. These clay-like materials undergo brittle-ductile transitions due to changes in salt content, i.e. changes in interparticle interactions. [12] Issues of brittleness and ductility are also crucial for the production of high-strength polycrystalline metallic alloys in which such transitions have been studied experimentally with respect to temperature and loading rate. [13] My immediate goal is to identify those molecular-level phenomena which must undergo further investigation in a larger project of understanding what makes one amorphous material ductile while another material or even the same material under different conditions may be brittle.

I describe here two computer simulations, one displaying brittle behavior and, the other, ductile behavior. In

these simulations, a modest change in inter-atomic potential was responsible for a qualitative difference in the means of crack propagation: atomic scale cleavage in the brittle case, blunting followed by void nucleation and growth in the ductile case. This change in behavior resulted in a corresponding jump in fracture toughness. In order to make a connection between a dislocation-like molecular process which may occur in a non-crystalline system and the observed change in fracture toughness and propagation mechanism, I have developed a measure of non-affine rearrangement which identifies the regions that have undergone plastic deformation.

The simulated systems consisted of 90,000 particles in two-dimensions interacting via a two-body potential. In order to avoid problems of local crystallization, a polydisperse collection of particles was simulated. The system was composed of eight different species in equal proportion with radii from approximately 0.34 to 0.67 units. The radius of each species was 10% larger than the next smallest, and the total volume of the collection was the same as if the particles were all of radius 0.5. This was done to make the system roughly comparable to a single component system in which the rest spacing between two molecules is $r_0 = 1$. The masses of all particles were taken to be $m = 1$.

The inter-molecular potential was different in the two simulations. In the ductile simulation the potential was a standard Lennard-Jones 6-12 potential

$$U_{\alpha\beta}^{LJ}(r) = e \left[\left(\frac{r_\alpha + r_\beta}{r} \right)^{12} - 2 \left(\frac{r_\alpha + r_\beta}{r} \right)^6 \right], \quad (1)$$

where r is the interparticle distance and r_α and r_β are the radii of the two particles. e , the depth of the energetic minimum of the two particle interaction, was chosen to be unity. In the brittle simulation a different potential was used. I will refer to this potential as a Compressed Lennard-Jones potential because it is the standard Lennard-Jones potential rescaled around the center of the potential well,

$$U_{\alpha\beta}^{CLJ}(r) = U_{\alpha\beta}^{LJ}(\lambda r + (1 - \lambda)(r_\alpha + r_\beta)). \quad (2)$$

The parameter λ was chosen to be 1.5. This means that width of the potential well was smaller by 33%, and,

consequently, the effective range of interaction was also shortened compared to the standard 6-12 Lennard-Jones interaction. In both cases interactions were cut off at a range of $\approx 2.2r_0$.

All times are given in units of $t_0 = r_0 \sqrt{m/e}$. This unit of time is approximately equivalent to one molecular vibrational period.

The initial amorphous systems were created by taking 10,000-molecule systems and equilibrating them using a sequential MD algorithm with periodic boundary conditions, a Nose-Hoover thermostat [14–16] and Parrinello-Rahman barostat [17,18]. The timestep in the simulation was taken to be 0.01 time units. The systems were quenched at low temperature while simultaneously being subjected to high pressures in order to create close-packed samples. The samples were then allowed to relax to zero pressure. The ductile sample was observed to have a Young's modulus of 34.9; the brittle sample was observed to have a Young's Modulus of 41.3. Here the moduli are given in units of e/r_0^2 . The Poisson ratio in both samples was observed to be 0.63. Note that in a two-dimensional system, unlike a three-dimensional system, the maximum Poisson ratio is 1.0. These 10,000-molecule samples were then used to create larger systems by replicating the small system in a 3×3 array.

The larger systems were simulated via a parallel MD algorithm based on a spatial decomposition method. [19] In order to create the initial conditions for the fracture simulations, the large system was equilibrated for 100 time units while held at a very low temperature, $kT = 0.001e$. A crack was then introduced into the sample. This was accomplished by imposing displacements as determined by the analytical solution for a straight crack in an elastic medium loaded below the ideal critical stress. The faces of the crack were marked so that the top face would not interact with the bottom face to prevent the crack from healing. The outer boundaries of the system were constrained while the simulation was again run to allow the system to relax, holding the temperature constant.

In the fracture simulations no thermostat or barostat was employed. To drive the crack, an initial velocity gradient was imposed across the sample, and the top and bottom surfaces were constrained to move apart vertically such that the side closer to the crack would separate at a strain rate of $0.0001t_0^{-1}$ and the side farthest from the crack would not move apart at all. The horizontal motion of these surfaces was unconstrained. The left and right surfaces were constrained not to move in the horizontal direction, though their vertical motion was unconstrained.

A strain rate of $0.0001t_0^{-1}$ corresponds to a physical strain rate on the order of $10^8 s^{-1}$. While this may seem high compared to typical laboratory values, we can ascertain if there is time for the stresses to equilibrate by multiplying this rate by the time for a sound wave to

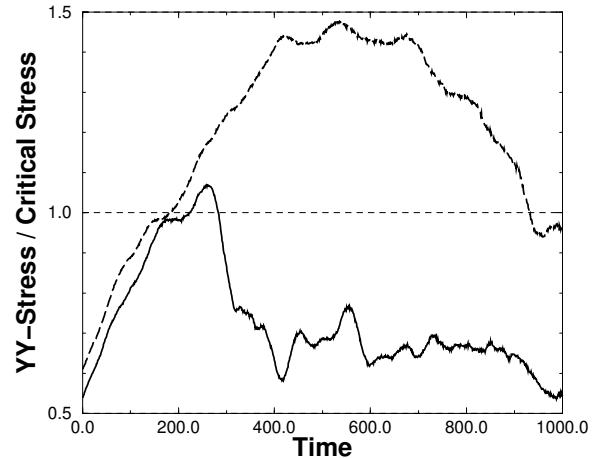


FIG. 1. Stress averaged throughout the sample versus time for the brittle (solid) and ductile (dashed) simulations. The higher stress for the onset of fracture in the ductile case implies increased dissipation. Stresses are given in units of the critical stress for failure of an ideally brittle material with the same elastic properties. Time is given in units of $r_0 \sqrt{m/e}$.

traverse the sample, $\approx 300t_0$. The fact that this number is $\approx 0.03 \ll 1$ implies that the system is, in this sense, being loaded nearly quasi-statically. That is to say that the loading rate is much slower than the elastic response time, although the loading may not be slow when compared to the time scale for plastic response. Of course, if the crack begins to propagate strain rates near the tip may be significantly higher.

Figure 1 shows the average stress measured during both the brittle and the ductile simulations. In order to better compare the two systems, the stresses are given in units of the critical stress for initial failure of a perfectly brittle solid with the identical elastic properties,

$$\sigma_c = \sqrt{\frac{GE}{\pi a}}. \quad (3)$$

Here we assume that, to a good approximation, the system can be treated as a crack in an infinite medium. E is Young's Modulus; a is the initial length of the crack; and G is the energy release rate, which can be expressed as a surface energy and a dissipation per unit crack extension,

$$G = 2\gamma + G_{diss}. \quad (4)$$

For an ideally brittle solid all the elastic energy released goes into the creation of new surface, $G_{diss} = 0$. γ was measured by taking a sample of the material in MD, slicing it along an arbitrary plane and measuring the change in potential energy. The value of γ is 1.04 in the ductile system and 0.94 in the brittle system in units of e/r_0 , thus $\sigma_c^{ideal} = 0.68$ in the ductile system and 0.70 in the brittle system.

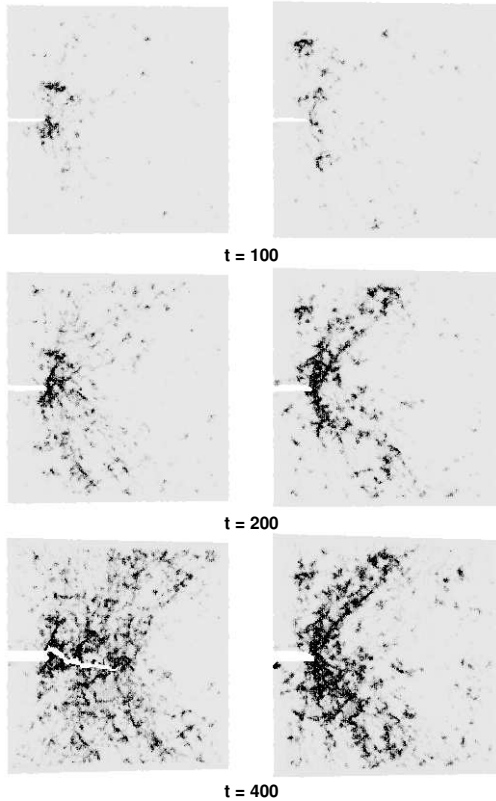


FIG. 2. Frames from the brittle (left) and ductile (right) fracture simulations. In each set the frames are shaded by the parameter D_{min}^2 defined in Eq. 5. Dark regions have undergone the highest amount of non-affine rearrangement. The shading saturates when $D_{min}^2 = 1$.[†]

Two notable differences are observed between the simulations: (i) In the brittle simulation, some modest amount of energy has been dissipated and the crack begins to propagate at about 7% above the ideal brittle critical stress, but in the ductile simulation fracture does not proceed until the stress is 48% above this value. This means that for the brittle case the ratio of energy dissipated to the energy expended creating surface is 0.14, while for the ductile case this ratio is 1.19. (ii) In the brittle simulation, once the crack begins to propagate, the stress in the system sharply dips as the crack moves through the system at speeds reaching 30% of the shear wave speed. Throughout this process the crack tip remains atomically sharp. The process stops short of releasing all the stress because the crack arrests. In the ductile case, however, the crack tip blunts significantly. In this simulation, the stress remains high while voids nucleate ahead of the tip. The speed of the ductile crack,

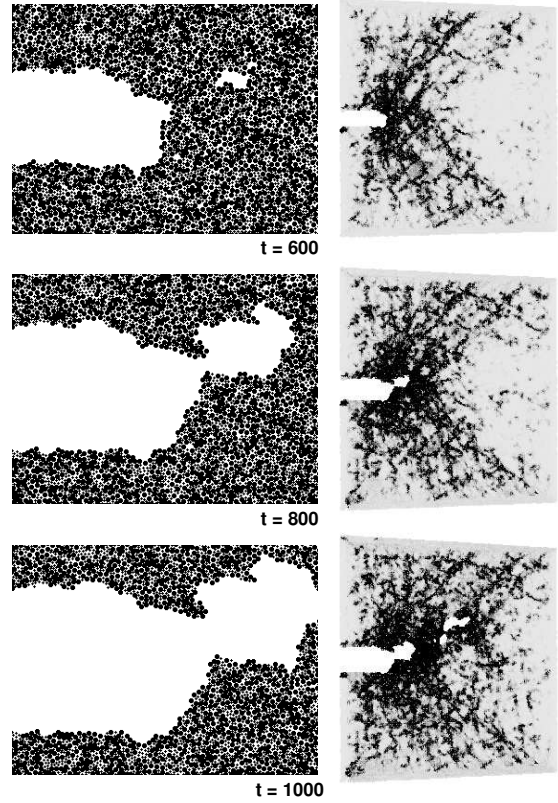


FIG. 3. Frames from the ductile simulation showing the nucleation and growth of a void in the vicinity of the crack tip. The frames on the left are close-ups of the crack tip. The frames on the right are shaded as in Figure 2.[†]

while difficult to measure due to the mechanism of propagation, stays well below the speed of the brittle crack.

If the simulations carried out here had been performed in crystals [20,21] we would be interested in identifying the dislocations which had been emitted from the crack tip or activated in the vicinity of the crack. In a perfect crystal, dislocations can be readily identified by their characteristic stress fields or as regions of anomalously high potential energy. In glasses, however, such analyses are difficult due to inhomogeneities frozen into the structure. Furthermore, it is not clear that any analog of crystalline dislocations exists in non-crystalline solids. For these reasons, we need some means of identifying regions which deform in a non-affine way in order to observe what sort of microscopic structures play the role of dislocations in these materials.

For the purpose of identifying local rearrangements, let us define a quantity D_i^2 , the deviation from a local affine

[†]Quicktime movies of these simulations can be found at <http://golem.physics.ucsb.edu/~mikefalk/research.html>

strain, ε , in the vicinity of a particle, i ,

$$D_i^2 = \sum_{\alpha} \sum_{j \neq i} \left[u_{\alpha}^j - u_{\alpha}^i - \sum_{\beta} \varepsilon_{\alpha\beta} (R_{\beta}^j - R_{\beta}^i) \right]^2, \quad (5)$$

where u_{α}^i is the α component of the displacement of particle i from its initial position; and R_{α}^i is the α component of the initial position of particle i . We can then define D_{min}^2 as the above quantity minimized with respect to ε .

The right-hand frames in Figures 2 and 3 are shaded by the value of D_{min}^2 . It is immediately apparent that much more non-affine rearrangement takes place in the ductile simulation than in the brittle simulation. In addition, there seem to develop preferred directions along which deformation takes place. These slip bands which nucleate at the crack tip in the ductile simulation are clear signs that the dynamics of the plastic response and the resulting propagating shear modes are crucial aspects of the problem.

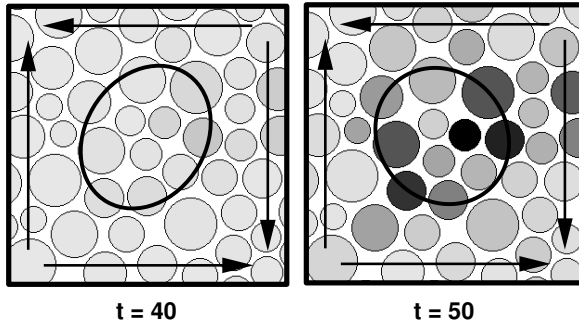


FIG. 4. A local region before and after non-affine rearrangement. The molecules are shaded by D_{min}^2 , the amount of non-affine rearrangement. The arrows denote the approximate direction of the externally applied shear. The ovals are included solely as guides for the eye.

Figure 4 shows one example of a local region before and after rearrangement. This rearrangement took place in the early stages of the ductile simulation prior to significant blunting a small distance in the y -direction from the tip. The arrows denote the sense of the externally applied shear in this region calculated by knowing the asymptotic stress field near a crack tip. The figure illustrates that these regions appear to be of the type discussed by Spaepen as “flow defects.” [22–26] That is, the region seems to consist of roughly 10–20 particles, the rearrangements seem to be local, and the “defect” is not mobile in the same sense as a dislocation.

The simulations suggest that deformation composed of small local transformations of the type illustrated in Figure 4 are responsible for the plastic response of amorphous materials. The activation of these transformations is affected by the inter-atomic potential, but is also likely to be sensitive to rate effects, temperature and local ordering. It is also apparent from these simulations that the

dynamics of the plastic response governed by these microscopic events controls whether a crack will propagate in a brittle or ductile manner. In order to understand the underlying physics of this plastic response, further investigations have been undertaken to characterize the dynamics of these regions. These results are being reported separately. [27]

I would like to acknowledge J.S. Langer for his guidance and encouragement, and A.S. Argon, B.L. Holian, M. Marder and R.L.B. Selinger for helpful discussions. This work was supported by the DOE Computational Sciences Graduate Fellowship Program and DOE Grant No. DE-FG03-84ER45108. The work was also supported in part by National Science Foundation grant CDA96-01954, Silicon Graphics Inc., and the Cornell Theory Center.

- [1] J. Rice and R. Thomson, *Phil. Mag.* **29**, 73 (1974).
- [2] J. Rice, *J. Mech. Phys. Solids* **40**, 239 (1992).
- [3] S. Zhou, A. Carlsson, and R. Thomson, *Phys. Rev. Lett.* **72**, 852 (1994).
- [4] L. Freund and Y. Lee, *Int. J. Frac.* **42**, 261 (1990).
- [5] E. Glennie, *J. Mech. Phys. Solids* **19**, 255 (1971).
- [6] J. Langer and A. Lobkovsky, to be published, *J. Mech. Phys. Solids*.
- [7] E. Hart, *Int. J. Solids Struct.* **16**, 807 (1980).
- [8] L. Freund and J. Hutchinson, *J. Mech. Phys. Solids* **33**, 169 (1985).
- [9] W. Johnson, *Mat. Sci. Forum* **225**, 35 (1996).
- [10] C. Gilbert, R. Ritchie, and W. Johnson, *App. Phys. Lett.* **71**, 476 (1997).
- [11] T.-W. Wu and F. Spaepen, *Phil. Mag. B* **61**, 739 (1990).
- [12] G. Franks and F. Lange, *J. Am. Ceramic Soc.* **79**, 3161 (1996).
- [13] R. Noebe, C. Cullers, and R. Bowman, *J. Mater. Res.* **7**, 605 (1992).
- [14] S. Nose, *J. Chem. Phys.* **81**, 511 (1984).
- [15] S. Nose, *Molec. Phys.* **52**, 255 (1984).
- [16] S. Nose, *Molec. Phys.* **57**, 187 (1986).
- [17] M. Parrinello and A. Rahman, *J. Appl. Phys.* **52**, 7182 (1981).
- [18] M. Parrinello and A. Rahman, *J. Chem. Phys.* **76**, 2662 (1982).
- [19] S. Plimpton, *J. Comp. Phys.* **117**, 1 (1995).
- [20] S. Zhou, P. Lomdahl, R. Thomson, and B. Holian, *Phys. Rev. Lett.* **76**, 2318 (1996).
- [21] F. Abraham, D. Brodbeck, R. Rafey, and W. Rudge, *Phys. Rev. Lett.* **73**, 272 (1994).
- [22] F. Spaepen, *Acta metall.* **25**, 407 (1977).
- [23] A. Argon, *Acta metall.* **27**, 47 (1979).
- [24] A. Argon and H. Kuo, *Mat. Sci. Eng.* **39**, 101 (1979).
- [25] F. Spaepen and A. Taub, in *Les Houches Lectures XXXV on Physics of Defects*, edited by J.-P. P. R. Balian, M. Kleman (North-Holland, Amsterdam, 1981), p. 133.

[26] A. Argon and L. Shi, *Acta metall.* **31**, 499 (1983). [27] M. Falk and J. Langer, to be published, *Phys. Rev. E*.